Inorganic Chemistry Communications 63 (2016) 74–80

Contents lists available at ScienceDirect

Inorganic Chemistry Communications

journal homepage: www.elsevier.com/locate/inoche

Short communication

Anti-*Mycobacterium tuberculosis* activity of platinum(II)/*N*,*N*-disubstituted-*N*′-acyl thiourea complexes

Ana M. Plutín [a,*], Anislay Alvarez [a], Raúl Mocelo [a], Raúl Ramos [a], Eduardo E. Castellano [b], Monize M. da Silva [c], Legna Colina-Vegas [c], Fernando R. Pavan [d], Alzir A. Batista [c,*]

[a] Facultad de Química, Universidad de La Habana, La Habana, Cuba
[b] Instituto de Física de São Carlos, Universidade de São Paulo, São Carlos, SP, Brazil
[c] Departamento de Química, Universidade Federal de São Carlos, São Carlos, SP, Brazil
[d] Faculdade de Ciências Farmacêuticas, UNESP, Araraquara, SP, Brazil

ARTICLE INFO

Article history:
Received 31 July 2015
Accepted 29 November 2015
Available online 4 December 2015

Keywords:
Platinum(II) complexes
1,1′-Bis(diphenylphosphino)ferrocene
N,*N*-Disubstituted-*N*′-acyl thioureas
Anti-*Mycobacterium tuberculosis* assays

ABSTRACT

Synthesis, characterization and anti-*Mycobacterium tuberculosis* assays of new platinum(II)/dppf/*N*,*N*-disubstituted-*N*′-acyl thiourea complexes with general formulae [Pt(dppf)(L)]PF_6, [dppf = 1,1′-bis(diphenylphosphino)ferrocene; L = *N*,*N*-disubstituted-*N*′-acyl thioureas] is reported. The complexes were characterized by elemental analysis, molar conductivity, IR, NMR (^{1}H, ^{13}C and ^{31}P{^{1}H}) spectroscopy. The spectroscopic data are consistent with the complexes containing one dppf and one O, S chelated ligand. The crystal structures of complexes with *N*,*N*-diphenyl-*N*′-benzoylthiourea **(L4)**, *N*,*N*-diethyl-*N*′-furoylthiourea **(L5)** and *N*,*N*-diphenyl-*N*′-(thiophene-2-carbonyl)thiourea **(L8)** were determined by X-ray crystallography, confirming the coordination of the ligands with the metal through sulfur and oxygen atoms, forming distorted square-planar structures. The complexes were screened with respect to their anti-*M. tuberculosis* activity (H37Rv ATCC 27294).

1. Introduction

Thiourea and its derivatives act as chelating agents [1] and have found extensive applications in the fields of medicine, agriculture and analytical chemistry. These compounds exhibit a wide variety of biological activities, such as antiviral, antibacterial, antifungal [2], antitubercular, herbicidal, and insecticidal [3]. They are also involved in catalysis [4], and in anion recognition [5]. Coordination compounds of thiourea have been studied for various biological systems with respect to antibacterial, antifungal and anticancer activities [6]. Moreover, luminescence properties of a series of Pt(II) complexes bearing *N*-benzoylthiourea derivatives have been investigated, which find applications in optoelectronic devices, luminescent probes for biomolecules and chemical sensors [7]. More recently, there have been efforts to design non-classical platinum-acylthiourea complexes in order to investigate their antifungal activity and inhibitory activities against viruses [8].

Here we report the synthesis, characterization and anti-*Mycobacterium tuberculosis* activity of new platinum(II) complexes containing 1,1′-bis-(diphenylphosphino)ferrocene and *N*,*N*-disubstituted-*N*′-acyl thioureas as ligands. The *N*,*N*-disubstituted-*N*′-acyl thioureas used as ligands in this work were synthesized by the procedure previously reported [9], following the Scheme 1 below, by reacting methanolic solutions of acylthioureas with the precursor, dichloro[1,1′-bis(diphenylphosphino)ferroceno]platinum(II). The coordination between acylthiourea derivatives and the precursor proceeded by an exchange reaction, which involved deprotonation of the acyl thioureido group of the ligands during the complexes formation [10].

2. Experimental

2.1. Material and measurements

The dichloro[1,1′-bis(diphenylphosphino)ferrocene]platinum(II) was obtained from Strem. All reagents were purchased with reagent grade and used without further purification. Solvents were dried and used freshly distilled, unless otherwise specifically indicated. Thin layer chromatography (TLC) was performed on 0.25 mm silica gel precoated plastic sheets (40/80 mm) (Polygram_SIL G/UV254, Macherey & Nagel, Düren, Germany) using benzene/methanol (9/1) as eluent. The IR spectra were recorded on a FTIR Bomem-Michelson 102 spectrometer in the 4000–200 cm^{-1} region using CsI pellets. Conductivity values were obtained using 1.0 mM solutions of complexes in CH_2Cl_2, using a Meter Lab CDM2300 instrument. ^{1}H, ^{31}P{^{1}H} and ^{13}C NMR spectra, were recorded in $CDCl_3$, on a Bruker DRX 400 MHz. The ^{1}H chemical shifts are referenced to TMS. The ^{31}P{^{1}H} shifts are reported in relation

* Corresponding authors.

http://dx.doi.org/10.1016/j.inoche.2015.11.020
1387-7003/

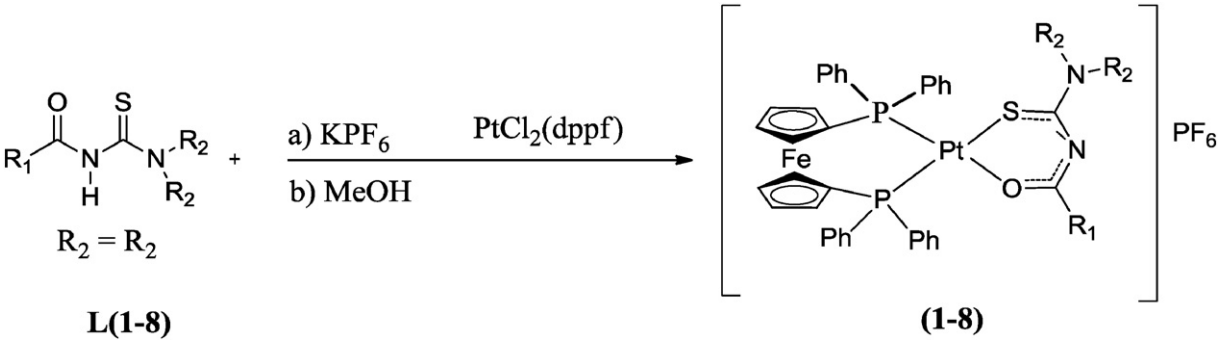

Scheme 1. Pathway for the synthesis of Pt(II)/*N*,*N*-disubstituted-*N*′-acyl thiourea complexes.

to H_3PO_4, 85%. Elemental analyses were carried out in an FISONS instrument, CHNS EA-1108.

2.2. Synthesis of *N*,*N*-disubstituted-*N*′-acyl thioureas

The *N*,*N*-disubstituted-*N*′-acyl thioureas L(1–8) used in this work were synthesized as crystalline solids, in good yields, by the procedure previously reported in the literature [9]. A solution of an appropriately acyl chloride (30 mmol) in acetone (50 mL) was added, drop wise, to a suspension of KSCN (0.01 mol) in acetone (30 mL). The mixture was stirred until a precipitate appeared (ammonium chloride), indicating the formation of the respective organic isothiocyanate. The corresponding amine (40 mmol), dissolved in acetone (20 mL) was slowly added to the reaction flask, with constant stirring. The solution was cooled in an ice-water bath and the stirring was continued, at room temperature, during 2–9 h longer, until the reaction was completed (the reaction progress was monitored by TLC). The reaction mixture was then poured into cold water (20 mL). Solids of *N*,*N*-disubstituted-*N*′-acyl thioureas were collected by filtration and finally purified by recrystallization from methanol. The identity of the products was confirmed by comparing their ^{1}H and ^{13}C NMR data with those reported in the literature [9]. Scheme 2 shows the pathway for the synthesis of the thioureas and the structures of the ligands are shown in Fig. 1.

2.3. Synthesis of the complexes

The complexes were prepared by a similar method used for $[Pd(PPh_3)_2Cl_2]$ [11] from direct reactions of the precursor $[Pt(dppf)Cl_2]$, with the *N*,*N*-disubstituted-N′-acyl thioureas, in methanol solutions. The complexes were separated from the reaction mixtures as white crystalline solids. Filtration and further washing with hot water and diethyl ether were enough to afford pure and stable compounds, with yields at about 80%. Thus, the general procedure for the synthesis of the complexes is described: a solution of $[Pt(dppf)Cl_2]$ (164 mg; 0.2 mmol) in 5 mL of methanol, was added dropwise to a solution of the corresponding *N*,*N*-dialkyl-*N*′-acyl thiourea ligand (0.2 mmol), dissolved in 30 mL of the same solvent. To this solution KPF_6 (368 mg, 2 mmol) was added. The reaction mixture was heated under magnetic stirring at 80 °C, for 2 h. After this time the reaction mixture was cooled

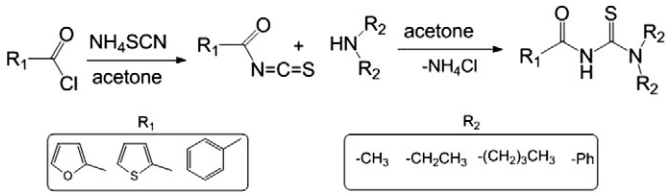

Scheme 2. Pathway for the synthesis of the *N*,*N*-disubstituted-*N*′-acyl thioureas.

down, and left in the refrigerator overnight. The obtained yellow solids were filtered off and washed, successively, with hot water and diethyl ether (3 × 20 mL). The obtained compounds are stable in the air.

The ^{1}H and ^{13}C NMR data, the elemental analyses, melting point temperature and molar conductivity (Λ_m, 1.0×10^{-3} mol/L, in CH_2Cl_2) for the complexes are listed below and the other data used for the characterization of the complexes are in the text:

(1) [Pt(dppf)(*N*,*N*-dimethyl-*N*′-benzoylthioureato-k^{2}O,S)]PF_6

Anal. calcd for $C_{45}H_{42}F_6FeN_2OP_3PtS_2$, (%): exp. (cal) C, 47.86 (47.97); H, 3.65 (3.57); N, 2.43 (2.54); S, 2.94 (2.91).

^{1}H NMR ppm: 7.86–7.81 (m; 5 H; Ph); 7.64–7.51 (m; 5 H); 7.37–7.17 (m; 10 H); 3.48 (3 H; s; CH_3) and 3.18 (3 H; s; CH_3). NMR ^{13}C ppm: 169.69 (CS); 161.84 (CO); 134.49, 134.42, 134.37, 134.23, 134.11, 132.75–127.73 (C-Ph); 29.70 (CH_3); 15.27 (CH_3); ^{31}P{^{1}H}}: 21.10 (d) and 9. 86 (d); $^2J_{P\text{-}P} = 23.48$ Hz. IR: ν(CO) 1437; ν(CS) 748; ν(CN) 1505; Anal. (%): Found (Calc): C, 60.38 (60.35); H, 4.30 (4.25); N, 2.35 (2.37); S, 2.70 (2.82). MP: 262–264 °C. $\Lambda_M = 49.6\ \Omega^{-1}\ cm^2\ mol^{-1}$.

(2) [Pt(dppf)(*N*,*N*-diethyl-*N*′-benzoylthioureato-k^{2}O,S)]PF_6

Anal. calcd $C_{47}H_{46}F_6FeN_2OP_3PtS_2$, (%): exp. (cal) C, 48.76 (48.90); H, 3.85 (3.84); N, 2.43 (2.48); S, 2.74 (2.84).

^{1}H NMR ppm: 7.87–7.82 (m; 1 H); 7.61–7.48 (m; 5 H); 7.36–7.31 (m; 5 H); 7.15–6.99 (m; 10 H); 3.81 (d; $J = 7.07$ Hz; 2 H; CH_2); 3.58 (d; $J = 7.07$ Hz; 2 H; CH_2); 1.28 (t; $J = 7.02$ Hz; 3 H; CH_3), 1.31 (t; $J = 7.02$ Hz; 3 H; CH_3); NMR ^{13}C ppm: 168.20 (CS); 166.22 (CO); 135.65, 135.59, 134.60, 134.49, 134.23–127.50 (C-Ph); 47.46 (CH_2); 46.53 (CH_2); 13.15 (CH_3); 12.01 (CH_3); ^{31} P{^{1}H}: 20.85 (d) and 10.19 (d); $^2J_{P\text{-}P} = 24.29$ Hz. IR: ν(CO) 1436; ν(CS) 750; ν(C = N) 1503. MP: 272–274 °C. $\Lambda_M = 45.6\ \Omega^{-1}\ cm^2\ mol^{-1}$.

(3) [Pt(dppf)(*N*,*N*-dibuthyl-*N*′-benzoylthioureato-k^{2}O,S)]PF_6

Anal. calcd for $C_{51}H_{54}F_6FeN_2OP_3PtS_2$, (%): exp. (cal) C, 50.46 (50.64); H, 4.45 (4.33); N, 2.43 (2.36); S, 2.64 (2.70).

^{1}H NMR ppm: 8.04–7.99 (m; 1 H); 7.80–7.08 (m; 34 H); 4.88 (d; J = 7.08 Hz; 2 H, CH_2); 3.68 (4 H; q; CH_2); 2.07–1.70 (2 H; m; CH_2); 0.93 (t; 3H, —CH_3; $J = 7.01$ Hz). NMR ^{13}C ppm: 168.90 (CS); 167.91 (CO); 135.55, 135.32, 135.21, 133.56–128.82 (C-Ph); 53.58 (CH_2); 52.38 (CH_2); 20.86 (CH_2); 14.20 (CH_3); ^{31}P{^{1}H}: 20.97 (d) and 10. 14 (d); $^2J_{P\text{-}P} = 22.67$ Hz. IR: ν(CO) 1436; ν(CS) 747; ν(CN) 1500. MP: 232–234 °C. $\Lambda_M = 49.6\ \Omega^{-1}\ cm^2\ mol^{-1}$.

(4) Pt(dppf)(*N*,*N*-diphenyl-*N*′-benzoylthioureato-k^{2}O,S)]PF_6

Anal. calcd for $C_{54}H_{43}F_6FeN_2OP_3PtS$], (%): exp. (cal) C, 52.96 (52.91); H, 3.74 (3.54); N, 2.33 (2.29); S, 2.64 (2.62).

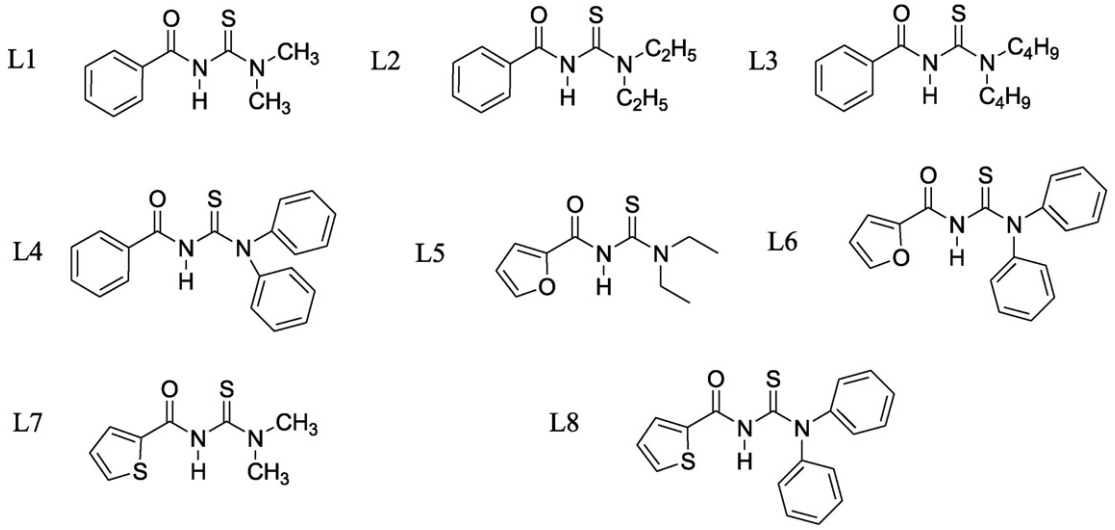

Fig. 1. Structures of the *N,N*-disubstituted-*N′*-acyl thioureas ligands used in this work.

^{1}H NMR ppm: 7.86–7.82 (m; 1 H); 7.14 (s; 1 H); 6.73 (d; $J = 1.60$ Hz; 1 H), 6.86–6.83 (m; 1 H). NMR ^{13}C ppm: 170.81. (CS); 168.48 (CO); 144.03, 143.08, 134.37, 134.26, 134.22, 134.10–127. 27 (C\Ph). ^{31}P{^{1}H}: 20.77 (d) and 9.77 (d); $^{2}J_{P\text{-}P} = 22.67$ Hz. IR: ν(CO) 1428; ν(CS) 750; ν(CN) 1485. MP: 272–276 °C. $\Lambda_M = 50.6\ \Omega^{-1}\ cm^2\ mol^{-1}$.

(5) [Pt(dppf(*N,N*-diethyl-*N′*-furoylthioureato-k^{2}O,S)]PF_6

Anal. calcd for $C_{44}H_{41}F_6FeN_2O_2P_3PtS$, (%): exp. (cal) C, 47.26 (47.20); H, 3.65 (3.69); N, 2.43 (2.50); S, 2.84 (2.86).

^{1}H NMR ppm: 7.85–7.80 (m; 1H), 7.60–6.18 (3H; m; furoyl), 3.74 (2H; c; CH_2), 3.34 (2H; c; CH_2); 1.22 (3H; t; CH_3); 0.95 (3H; t; CH_3). NMR ^{13}C ppm: 165.67 (CS); 159.79 (CO); 145.90, 134.58, 134.47, 134.12–129.38 (C-Ph); 128.80–112.04 (C-Ph and furan ring); 47.17 (CH_2); 46.48 (CH_2); 13.11 (CH_3) 11.90 (CH_3).^{31} P{^{1}H}: 20.44 (d) and 10.34 (d); $^{2}J_{P\text{-}P} = 20.34$ Hz. IR: ν(CO) 1423; ν(CS) 758; ν(CN) 1483. MP: 246–248 °C. $\Lambda_M = 49.6\ \Omega^{-1}\ cm^2\ mol^{-1}$.

(6) [Pt(dppf)(*N,N*-dibenzyl-*N′*-furoylthioureato-k^{2}O,S)]PF_6

Anal. calcd for $C_{53}H_{44}F_6FeN_2OP_3PtS_2$, (%): exp. (cal) C, 52.26 (52.14); H, 3.68 (3.65); N, 2.33 (2.25); S, 2.54 (2.58).

^{1}H NMR ppm: 7.91–7.80 (m; 1H); 7.63–7.43 (m; 1H); 7.20–6.99 (m; 1H), 6.53–6.16 (m; 1H); 4.98 (s; 2H; CH_2); 4.77 (s; 2H; CH_2) PPM. NMR ^{13}C ppm: 167.74 (CS); 161.98 (CO); 149.50, 146.75, 146.14, 145.72, 145.23–112.28 (C-Ph); 53.47 (CH_2); 52.78 (CH_2). ^{31}P{^{1}H}: 20.35 (d) and 9.80 (d); $^{2}J_{P\text{-}P} = 22.67$ Hz. IR: ν(CO) 1528; ν(CS) 752; ν(CN) 1578. MP: 266–268 °C. $\Lambda_M = 52.6\ \Omega^{-1}\ cm^2\ mol^{-1}$.

(7) [Pt(dppf)(*N,N*-dimethyl-N′-thiophenylthioureato-k^{2}O,S)]PF_6

Anal. calcd for $C_{43}H_{40}F_6FeN_2OP_2PtS_2$, (%): exp. (cal) C, 45.26 (45.54); H, 3.45 (3.37); N, 2.43 (2.53); S, 5.84 (5.79).

^{1}H NMR ppm: 7.87 (1 H; dd; $J1 = 7.2$ Hz; $J2 = 8.1$ Hz, Thiophene CH); 7.82 (1 H; dd, $J1 = 7.59$ Hz; $J2 = 8.2$ Hz, thiophene CH); 6.69 (1 H; dd; $J1 = 6.7$ Hz; $2 = 8.6$ Hz, thiophene CH), 7.59–7.57 (C-Ph); 0.97 (6H; t; $-CH_3$; $J = 7.1$ Hz), NMR ^{13}C ppm: 166.73 (CS); 164.10 (CO); 141.19, 134.57, 134.50, 134.47, 134.40, 132.3 8, 132.27, 132.18, 131.74, 128.90–125.62 (C-Ph); 21.80 ($2CH_3$). ^{31}P{^{1}H}: 20.90 (d) and 10.22 (d); $^{2}J_{P\text{-}P} = 22.67$ Hz. IR: ν(CO) 1437; ν(CS) 748; ν(CN) 1494. MP: 246–248 °C. $\Lambda_M = 49.6\ \Omega^{-1}\ cm^2\ mol^{-1}$.

(8) [Pt(dppf)(*N,N*-diphenyl-N′-thiophenylthioureato-k^{2}O,S)]PF_6

Anal. calcd for $C_{52}H_{41}F_6FeN_2OP_3PtS_2$, (%): exp. (cal) C, 50.85 (50.70); H, 3.45 (3.35); N, 2.23 (2.27); S, 2.84 (2.90).

^{1}H NMR ppm: 8.32 (1H; dd; $J1 = 7.2$ Hz; $J2 = 8.1$ Hz; Thiophene CH); 8.10 (1 H; dd; $J1 = 7.5$ Hz; $J2 = 8.2$ Hz; thiophene CH); 7.23 (1 H; dd; $J1 = 6.7$ Hz; $J2 = 8.3$ Hz; thiophene CH); 7.63–7.27 (m; 10 H; arom-H). NMR ^{13}C ppm: 167.04 (CS); 164.19 (CO); 134.60, 134.49, 134.17, 134.06, 132.71, 132.49, 132.24, 132.10, 129.42, 129.30, 128.53–127.83 (C-Ph); 25.28 ($2CH_3$). ^{31}P{^{1}H}: 20.66 (d) and 9. 99 (d); $^{2}J_{P\text{-}P} = 22.67$ Hz. IR: ν(CO) 1480; ν(CS) 747; ν(CN) 1590. MP: 255–257 °C. $\Lambda_M = 50.6\ \Omega^{-1}\ cm^2\ mol^{-1}$.

2.4. Crystal structure determination

Single crystals suitable for X-ray diffraction were obtained by slow evaporation of $CHCl_3$:n-hexane (3:1) solutions of the complexes **(4)**, **(5)** and **(8)**. Diffraction data were collected on an Enraf-Nonius Kappa-CCD diffractometer with graphite-monochromated Mo Ka radiation ($\lambda = 0.71073$ Å). The final unit cell parameters were based on all reflections. Data collections were performed using the COLLECT program [12]; integration and scaling of the reflections were performed with the HKL Denzo-Scalepack system of programs [13]. Absorption corrections were carried out using the Gaussian method [14]. The structures were solved by direct methods with SHELXS-97 [15]. The models were refined by full-matrix least-squares on F^2 by means of SHELXL-97 [16]. The projection views of the structures were prepared using ORTEP-3 for Windows [17]. Hydrogen atoms were stereochemically positioned and refined with the riding model. Data collections and experimental details are summarized in Table 1. Relevant interatomic bond lengths and angles are listed in Table 2.

2.5. Anti-M. tuberculosis activity assay

The anti-MTB activity of the compounds was determined by the REMA (Resazurin Microtiter Assay) method [18]. Stock solutions of the tested compounds were prepared in DMSO and diluted in Middlebrook 7H9 broth (Difco) supplemented with oleic acid, albumin, dextrose and catalase (OADC), performed by Precision XS (Biotek®) to obtain the final drug concentration range of 0.09–25 μg mL^{-1}. Isoniazid was dissolved in distilled water and rifampicin in DMSO, and both were used as standard drugs. A suspension of MTB H37Rv ATCC 27294 was cultured in Middlebrook 7H9 broth supplemented with OADC and 0.05% Tween 80. The cultures were frozen at −80 °C in aliquots. After two days the CFU per mL (colony formation unit per mL) of an aliquot was determined. The concentrations were adjusted by 5×10^5 CFU per mL and 100 μL of the inoculum were added to each well of a 96-well microplate together with 100 μL of the compounds. Samples

Table 1
Crystal data and refinement parameters of complexes **4**, **5** and **8**.

Compound	(4)	(5)	(8)
Empirical formula	$C_{54}H_{43}F_6N_2OP_3PtS$	$C_{44}H_{41}F_6FeN_2O_2P_3Pt\ S$	$C_{52}H_{41}F_6FeN_2OP_3PtS_2$
Formula weight	1225.81	1119.70	1231.84
Crystal system	Triclinic	Monoclinic	Triclinic
Space group	P − 1	P21/a	P − 1
a (Å)	12.2463(3)	10.8472(2)	12.5714(3)
b (Å)	13.5534(3)	28.8535(8)	13.7954(2)
c (Å)	15.8064(4)	14.0972(3)	15.0969(4)
α (°)	80.542(2)	90	96.074(2)
β (°)	77.027(2)	92.4280(10)	107.5660(10)
γ (°)	85.821(2)	90	91.973(2)
V (Å^3)	2520.05(11)	4408.18(17)	2476.03(10)
Z	2	4	2
D. calc (mg/m^3)	1.615	1.687	1.652
Absorption coefficient (mm^{-1})	3.260	3.720	3.359
F(000)	1216	2216	1220
θ range for data collection (°)	2.847 to 26.000	2.56 to 26.00	2.837 to 25.998
Index ranges	−15 ≤ h ≤ 15 −16 ≤ k ≤ 16 19 ≤ l ≤ 19	−13 ≤ h ≤ 12 −35 ≤ k ≤ 33 −13 ≤ l ≤ 17	−15 ≤ h ≤ 15 −17 ≤ k ≤ 17 −18 ≤ l ≤ 18
Reflections collected	28,024	28,060	31,475
Independent reflections (Rint)	9795 [R(int) = 0.0867]	8616 [R(int) = 0.0764]	9664 [R(int) = 0.0469]
Goodness-of-fit on F2	1.076	0.988	1.033
Final R indices	R1 = 0.0712	R1 = 0.0514	R1 = 0.0384
[I N 2σ (I)]	wR2 = 0.1815	wR2 = 0.1225	wR2 = 0.0978
Largest diff. peak and hole (eÅ)$^{-3}$	2.683 and −2.685	2.778 and −1.317	1.104 and −1.376

were set up in triplicate. The plates were incubated for 7 days at 37 °C. Resazurin (solubilized in water) was added (30 μL of 0.01%). The fluorescence of the wells was read after 24 h with a Cytation 3 (Biotek®). The MIC was defined as the lowest concentration resulting in 90% inhibition of growth of MTB.

3. Results and discussion

All the synthesized platinum(II) complexes are of yellow color, and their most useful infrared spectral bands for determining the ligands mode of coordination are given in Section 2, as well as the elemental analyses data, melting point temperatures, and molar conductivities. These data suggest the formation of complexes with the general formulae $[Pt(dppf)_2(L)]PF_6$, in which L represents the anionic ligand formed upon deprotonation, when the *N*,*N*-disubstituted-*N*′-acyl thioureas coordinate to the metal center.

The IR spectra of the ligands reveal broad and strong absorption bands in the range of 3053–3267 cm^{-1}, due to NH stretching vibrations. As expected, these bands, present in the free ligands, are absent in the IR spectra of the complexes. On the other hand, the ν(C—N) band, present in the complexes at 1483–1590 cm^{-1}, is absent in the free ligands, suggesting that when coordinated to the metal the nitrogen changes from sp^3 to sp^2 hybridization, as shown in Scheme 1. In agreement with the literature the coordination between the metal and carbonyl group, present in the thioureas, decreases of *ca.* 180 cm^{-1} the C—O stretching vibration frequency, when compared with the free ligand [19]. Thus, considering that the free ligands have their νCO bands at about 1680 cm^{-1}, it is reasonable to assign the bands in the range of 1428–1528 cm^{-1} to the coordinated CO group. The absorptions at 815–878 cm^{-1} in the spectra of free bases, *N*,*N*-disubstituted-*N*′-acylthioureas, attributed to the ν(C—S) stretching vibrations, shift to the 747–758 cm^{-1} range in the spectra of the complexes. This substantial change suggests deprotonation of the ligands, indicating coordination through the sulfur atom with a formally C—S single bond [20–23]. The absorptions at about 471 cm^{-1} in the IR spectra of the complexes can be assigned to the Metal-O vibration mode [24,25] and the assignment of the Pt—S stretching vibration bands at about 360 cm^{-1} are in accordance with the reported by Bayazeed H. Abdullah and others for platinum(II) complexes with s-donor ligands [26,27]. Thus, from the IR data it is possible to suggest that the *N*,*N*-disubstituted-*N*′-acyl thioureas are attached to the metal through the oxygen and sulfur, by a chelating system. The molar conductivity of the complexes, in CH_2Cl_2, show they are ionic species in the range of 1:1 electrolytes [28].

Table 2
Selected bond lengths (Å) and angles (°) for the complexes **(4)**, **(5)** and **(8)**.

	(4)	(5)	(8)
Bond lengths (Å)			
Pt–O	2.072(5)	2.034(4)	2.067(3)
Pt–P(2)	2.3227(19)	2.3228(16)	2.3232(10)
Pt–S	2.304(2)	2.3075(16)	2.3034(10)
Pt–P(1)	2.244(2)	2.2410(17)	2.2444(11)
S–C(1)	1.725(8)	1.736(7)	1.661(5
O–C(2)	1.272(9)	1.281(8)	1.273(5)
N(1)–C(2)	1.311(10)	1.306(9)	1.311(5)
N(1)–C(1)	1.372(10)	1.350(9)	1.361(5)
N(2)–C1	1.331(11)	1.348(8)	1.332(6)
Angles (°)			
O–Pt–S	91.06(15)	90.95(13)	91.97(8)
O–Pt–P(1)	178.77(17)	176.39(15)	178.76(10)
O–Pt–P(2)	84.22(15)	83.09(13)	82.87(8)
P(2)–Pt–S	174.32(7)	173.75(6)	173.64(4)
S–Pt–P(1)	88.73(8)	90.82(6)	88.16(4)
P(2)–Pt–P(1)	96.05(7)	95.24(6)	97.08(4)

The molecular structures of the complexes were also investigated by NMR (^{1}H, ^{13}C and ^{31}P{^{1}H}) spectroscopy and a comparative analysis on the basis of the spectroscopic data corresponding to both, free and coordinated ligands with the metallic ion, was carried out. The ^{1}H NMR data for the complexes are given in the experimental section. The ^{1}H NMR spectra of the free ligands show basically three sets of well separated signals corresponding to their R1, R2 substituents and to the NH proton. The signals of the NH protons appear as broad singlets in the region between 8.35 and 8.80 ppm [9]. The absence of the N—H proton after the coordination of the ligands to the metal is associated with an increase in electron density at the CN bond upon complexation [29,30]. A slight downfield shift was also observed in the aromatic protons and in the protons of the nitrogen substituents in the coordinated ligands, when compared to the chemical shift of the free ligands. The aromatic protons appear as a complex pattern in the region δ 8.32–6.16 ppm. In the ^{13}C NMR spectra the chemical shifts of the C—S carbon atoms of the ligands moved up field after their coordination to the metal for all complexes

studied, but in the case of the C—O group, this tendency was not observed for all complexes. The explanation for this is the fact that with the deprotonation of the secondary amide and with the formation of a "NC–S–Pt" species, the sulfur atoms, and consequently their neighbor carbon atoms, became more shielded in all complexes, something that does not happen with the carbon from the carbonyl group, to the same extent. The $^{31}P\{^{1}H\}$ NMR spectrum of the precursor [Pt(dppf)Cl_2], in CH_2Cl_2 solution, shows a singlet peak for phosphorous atoms at 13.06 ppm. For all complexes, in dimethyl sulfoxide solutions, two doublets arise, at about 20.53 and 9.83 ppm, indicating the presence of two magnetically different phosphorus atoms coordinated to the platinum(II) ion, all signals were flanked by satellite peaks of the respective multiplicity generated for the coupling of the phosphorus atoms with the isotope ^{195}Pt.

Also in the region of −138–158 ppm a multiple signal of the PF_6^- functioning as outer-sphere anions for the complexes obtained is observed, in accordance with the molar conductivity measurements for these complexes (see experimental section). These data are consistent with those obtained for some palladium(II) thiosemicarbazones and *N*,*N*-disubstituted-*N*′-acyl thioureas complexes [10,21]. The ^{1}H NMR

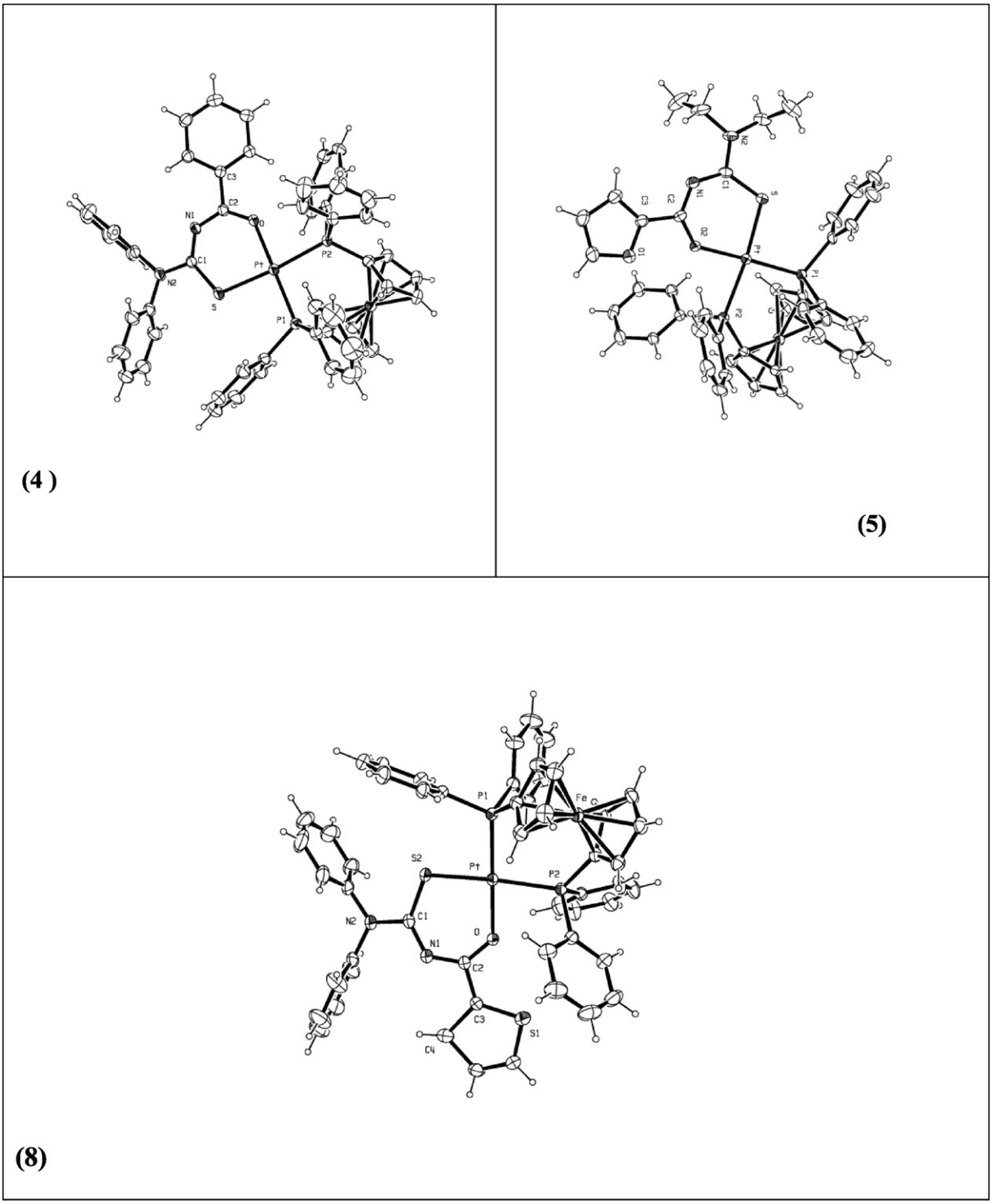

Fig. 2. ORTEP view of (4), (5) and (8) complexes showing 50% probability ellipsoids. Hydrogen atoms, the PF_6^- anion and some labels of the ligands are omitted for clarity.

integrations and signal multiplicities are consistent with [Pt(dppf)$_2$(L)]PF_6 structures for the complexes. All complexes are stable in dimethyl sulfoxide solutions, for at least 48 h, according to their NMR spectra in this solvent.

The structures of complexes **(4), (5)** and **(8)** were determined by X-ray diffraction analysis, and their ORTEP views are in Fig. 2 and selected bond lengths (Å) and angles (°) for the complexes are listed in Table 2. The thione C—S bond in the coordinated anionic ligands becomes formally a single bond making it longer (average = 1.707 Å) than the C—S bond of the neutral moieties [10], and the N(2)\C bond (average 1.337 Å), which some double bond in the anionic moieties, is typical for C—N distances [31]. The N(1)—C distance, 1.361 Å (average), is anionic and in the amine form. Thus the metal is coordinated to the negatively charged organic molecules, which act as bidentate ligands, through oxygen (average distance Pt–O = 2.058 Å) and through sulfur (average distance Pt—S = 2.304 Å) atoms. The Pt–S average distance is close to the ones found for other copper(II)/thiosemicarbazones complexes [23]. The remaining binding sites are occupied by dppf diphosphane ligand (average distance Pt–P1 = 2.243 Å and Pt–P(2) = 2.3229 Å). The distances for the C\S, C\N and C\O bonds in the chelate rings, listed in Table 2, are the characteristic of single and double bond lengths, respectively [31]. The CO bond distances are slightly sensitive to the coordination of the ligand to the metal. In the case of the bis-triphenylphosphine-*N*,*N*-diethyl-*N*′-furoilthioureato-k^{2}O,S the CO distance for the free ligand is 1.226(3) Å (average for two independent molecules per asymmetric unit), and 1.271(9) and 1.281(8) Å respectively, after its coordination to the metal [10].

3.1. Anti-*M. tuberculosis* activity

The compounds **(L1–L8)** and complexes **(1–8)** were investigated for their in vitro antimycobacterial activity against *M. tuberculosis* H37Rv strains, by the REMA. The minimum inhibitory concentrations (MICs) found for the platinum complexes, free ligands and ethambutol are shown in Table 3.

As can be seen from Table 3 results some compounds exhibited anti-*M. tuberculosis* activity, with reasonable low MIC values. Comparing the MIC values of the free *N*,*N*-disubstituted-*N*′-acyl thiourea with the values obtained for the complexes, it can be seen that the activity of the complexes is much higher than those of the uncoordinated *N*,*N*-disubstituted-*N*′-acyl thiourea, emphasizing the importance of the presence of the metal for anti-*M. tuberculosis* activity presented by the new complexes. Complexes **(1), (2), (5)** and **(7)** present approximately 10-fold and 20-fold higher activities, than the respective free *N*,*N*-disubstituted-*N*′-acyl thiourea.

The in vitro activity found for the complexes **(1), (2), (5)** and **(7)** is comparable to those of some commonly used anti-*M. tuberculosis* agents, like cycloserine (MIC = 122.4–489.7 μM), gentamicin (MIC = 4.19–8.38 μM), tobramycin (MIC = 8.56–17.11 μM), clarithromycin (MIC = 10.70–21.40 μM) and ethambutol (MIC = 5.62 μM), which is the clinically used as a first-line drug in several schemes of conventional tuberculosis treatment [32].

The structural changes in the ligands and in the complexes probably affect the interaction of the complexes with bacterial membrane. In our previous work with some ruthenium complexes it was suggested that the mechanism of their action against *M. tuberculosis* occurs in the cell wall biosynthesis [33]. This could be also a suggestion for the mechanism of the biological activity of the platinum complexes here studied, where the interaction of them with the mycobacterium membrane is modulated by the nature of the ligands present in the compounds.

Table 3
MIC values of antimycobacterial activity of Pt(II) complexes, free ligands and reference drug.

Compounds	μg/mL	μmol/L
L1	>25	˃119.61
L2	>25	˃107.30
L3	>25	˃85.62
L4	>25	˃75.30
L5	>25	˃110.62
L6	>25	˃75.30
L7	>25	˃116.82
L8	>25	˃73.96
(1) [Pt(dppf)(L1)]PF_6	5.49 ± 0.27	5.73 ± 0.28
(2) [Pt(dppf)(L2)]PF_6	6.51 ± 0.64	6.63 ± 0.65
(3) [Pt(dppf)(L3)]PF_6	23.66 ± 0.48	22.74 ± 0.46
(4) [Pt(dppf)(L4)]PF_6	>25	˃23.14
(5) [Pt(dppf)(L5)]PF_6	4.62 ± 0.06	4.74 ± 0.06
(6) [Pt(dppf)(L6)]PF_6	>25	˃23.14
(7) [Pt(dppf)(L7)]PF_6	5.76 ± 0.27	5.99 ± 0.28
(8) [Pt(dppf)(L8)]PF_6	>25	˃23.01
[Pt(dppf)Cl_2]	>25	˃30.47
Ethambutol	5.00	5.62

4. Conclusions

A novel series of Pt(II) complexes with *N*,*N*-disubstituted-*N*′-acyl thioureas as bidentate ligands was synthesized and thoroughly characterized by several spectroscopic techniques and X-ray crystallography. The X-ray crystallographic characterization shows that these ligands coordinate with the metal through the oxygen and sulfur atoms. The anti-*M. tuberculosis* activity assays of the new complexes provided evidence that they show activity against *M. tuberculosis* H37Rv, in the same order than the ethambutol, a first-line drug in several schemes of conventional tuberculosis treatment. Thus, as can been seen from Table 3, the MIC values are in order [Pt(dppf)(L5)]PF_6 < [Pt(dppf)(L1)]PF_6 < [Pt(dppf)(L7)]PF_6 < [Pt(dppf)(L2)]PF_6 < [Pt(dppf)(L3)]PF_6 < [Pt(dppf)(L4)]PF_6 ≈ [Pt(dppf)(L6)]PF_6 ≈ [Pt(dppf)(L8)]PF_6, showing that the most active complexes are those containing small R2 groups, like methyl or ethyl groups. Also, considering that the difference between complexes **(1)** and **(7)** is the R1 group and that their MIC values are practically the same, it is possible to suggest that this group does not influence substantially the activity of the complexes. The similar MIC values of complexes **(2)** and **(5)** give support to this suggestion. Shortly, the size of the R2 group influences the anti-*M. tuberculosis* activity of the [Pt(dppf)(Ln)]PF_6 complexes, which does not happen with the type of R1 group, at least in the same extend. Taken altogether, the influence of the R1 and R2 groups in the activity of the complexes can be due the steric hindrance or polarity in their interaction with the Mycobacterium membrane, affecting their cell wall biosynthesis. Thus, in this process the size of the R2 group plays a crucial role. The low antimycobacterial activity of the free ligands probably is due to their no interactions with the mycobacterium membrane.

Acknowledgments

This work was supported by CAPES (Project Oficio/CSS/CGCI/23038009487/2011-25/DRI/CAPES, AUX CAPES-MES-Cuba, 339/2011), CNPq and FAPESP (Process 2013/14957-5 and 2014/13691-4) of Brazil.

Appendix A. Supplementary data

CCDC 1405958, 1405957 and 1405956 contain the supplementary crystallographic data for Pt(dppf)(*N*,*N*-diphenyl-*N*′-benzoylthioureato-k^{2}O,S)]PF_6 **(4),** Pt(dppf(*N*,*N*-diethyl-*N*′-furoylthioureato-k^{2}O,S)]PF_6 **(5)** and Pt(dppf)(*N*,*N*-diphenyl-N′-thiophenylthioureato-k^{2}O,S)]PF_6 **(8),** respectively. These data can be obtained free of charge via http://www.ccdc.cam.ac.uk/conts/retrieving.html, or from the Cambridge Crystallographic Data Centre, 12 Union Road, Cambridge CB2 1EZ, UK; fax: (+44) 1223–336 033; or e-mail: deposit@ccdc.cam.ac.uk.

References

[1] H. Arslan, N. Duran, G. Borekci, C.K. Ozer, C. Akbay, Molecules 14 (2009) 519–527.
[2] S. Saeed, N. Rashid, R. Hussain, M. Ali, P.G. Jones, Eur. J. Med. Chem. 45 (2010) 1323–1331.
[3] Y.M. Zhang, T.B. Wei, L. Xian, L.M. Gao, Phosphorus Sulfur Silicon Relat. Elem. 179 (2004) 2007–2013.
[4] C.L. Gu, L. Liu, J.L. Zhao, D. Wang, Y.J. Chen, Tetrahedron 18 (2007) 455–463.
[5] S. Saeed, M.H. Bhatti, U. Yunus, P.G. Jones, Acta Crystallogr. E64 (2008) o1369.
[6] E. Maquoi, N.E. Sounni, L. Devy, F. Olivier, F. Frankenne, H.W. Krell, F. Grams, J.M. Foidart, A. Noel, Clin. Cancer Res. 10 (2004) 4038–4042.
[7] V. Cîrcu, M. Ilie, M. Iliş, F. Dumitraşcu, I. Neagoe, S. Păsculescu, Polyhedron 28 (2009) 3739–3746.
[8] S. Mihai, M. Negoiu, Rev. Chim. 63 (2012) 697–702.
[9] A. Plutin, H. Márquez, M. Morales, M. Sosa, L. Morán, Y. Rodríguez, M. Suárez, C. Seoane, N. Martín, Tetrahedron 56 (2000) 1533–1594.
[10] B. O'Reilly, A.M. Plutín, H. Pérez, O. Calderón, R. Ramos, R. Martínez, R.A. Toscano, J. Duque, H. Rodríguez-Solla, R. Martínez-Alvarez, M. Suárez, N. Martín, Polyhedron 36 (2012) 133–140.
[11] A.M. Plutín, R. Mocelo, A. Alvarez, R. Ramos, E.E. Castellano, M.R. Cominetti, A.E. Graminha, A.G. Ferreira, A.A. Batista, J. Inorg. Biochem. 134 (2014) 76–82.
[12] C. Enraf-Nonius, Nonius BV, Delft, The Netherlands, 1997–2000.
[13] Z. Otwinowski, W. Minor, Processing of X-ray diffraction data collected in oscillation mode, Macromol. Crystallogr. A 276 (1997).
[14] R.H. Blessing, Acta Crystallogr. Sect. A 51 (1995) 33–38.
[15] G.M. Sheldrick, ShelXS-97 Program for Crystal Structure Resolution, University of Göttingen, Göttingen, Germany, 1997.
[16] G.M. Sheldrick, SHELXL-97, Program for Crystal Structures Analysis, University of Göttingen, Göttingen, Germany, 1997.
[17] L.J. Farrugia, J. Appl. Crystallogr. 30 (1997) 565–566.
[18] J.C. Palomino, A. Martin, M. Camacho, H. Guerra, J. Swings, F. Portaels, Antimicrob. Agents Chemother. 46 (2002) 2720–2722.
[19] M. Mikami, I. Nakagawa, T. Shimanouchi, Spectrochim. Acta A 25 (1969) 365–374.
[20] A.E. Graminha, C. Rodrigues, A.A. Batista, L.R. Teixeira, E.S. Fagundes, H. Beraldo, Spectrochim. Acta A 69 (2008) 1073–1076.
[21] P.I.d.S. Maia, A.E. Graminha, F.R. Pavan, C.Q.F. Leite, A.A. Batista, D.F. Back, E.S. Lang, J. Ellena, S.d.S. Lemos, H.S. Salistre-de-Araujo, V.M. Deflon, J. Braz. Chem. Soc. 21 (2010) 1177–1186.
[22] A.P. Rebolledo, M. Vieites, D. Gambino, O.E. Piro, E.E. Castellano, C.L. Zani, E.M. Souza-Fagundes, L.R. Teixeira, A.A. Batista, H. Beraldo, J. Inorg. Biochem. 99 (2005) 698–706.
[23] A. Pérez-Rebolledo, L.R. Teixeira, A.A. Batista, A.S. Mangrich, G. Aguirre, H. Cerecetto, M. González, P. Hernández, A.M. Ferreira, N.L. Speziali, H. Beraldo, Eur. J. Med. Chem. 43 (2008) 939–948.
[24] K. Nakamoto, Infrared and Raman Spectra of Inorganic and Coordination Compounds, fourth ed. Wiley, New York, 1986.
[25] A. Pérez-Rebolledo, O.E. Piro, E.E. Castellano, L.R. Teixeira, A.A. Batista, H. Beraldo, J. Mol. Struct. 794 (2006) 18–23.
[26] B.H. Abdullah, Y.M. Salh, Orient. J. Chem. 26 (3) (2010) 763–773.
[27] M.N. Patel, C.R. Patel, H.N. Joshi, P.A. Vekariya, Appl. Biochem. Biotechnol. 172 (2014) 1846–1858.
[28] W.J. Geary, Coord. Chem. Rev. 7 (1971) 81–122.
[29] S. Ahmad, A.A. Isab, S. Ali, Transit. Met. Chem. 31 (2006) 1003–1016.
[30] S. Ahmad, Chem. Biodivers. 7 (2010) 543–566.
[31] H.H. Nguyen, J.J. Jegathesh, P.I.d.S. Maia, V.M. Deflon, R. Gust, S. Bergemann, U. Abram, Inorg. Chem. 48 (2009) 9356–9364.
[32] R.P. Tripathi, N. Tewari, N. Dwivedi, V.K. Tiwari, Med. Res. Rev. 25 (2005) 93–131.
[33] G.G.S. Leite, L.C. Baeza, A.A. Batista, M.I.F. Barbosa, F.R. Pavan, C.Q.F. Leite, J.L. Silva, R.D.C. Hirata, M.H. Hirata, R.F. Cardoso, Int. J. Microbiol. Res. 5 (1) (2013) 356–361.